Applied Nanoscience (2018) 8:1091–1099
https://doi.org/10.1007/s13204-018-0730-z

ORIGINAL ARTICLE

Enhanced photocatalytic performance of CeO_2–TiO_2 nanocomposite for degradation of crystal violet dye and industrial waste effluent

Mehvish Zahoor[1] · Amara Arshad[1] · Yaqoob Khan[2] · Mazhar Iqbal[1] · Sadia Zafar Bajwa[1] · Razium Ali Soomro[1] · Ishaq Ahmad[2] · Faheem K. Butt[3] · M. Zubair Iqbal[4] · Aiguo Wu[4] · Waheed S. Khan[1,4]

Received: 31 January 2018 / Accepted: 15 March 2018 / Published online: 20 March 2018

Abstract

This study presents the synthesis of CeO_2–TiO_2 nanocomposite and its potential application for the visible light-driven photocatalytic degradation of model crystal violet dye as well as real industrial waste water. The ceria–titania (CeO_2–TiO_2) nanocomposite material was synthesised using facile hydrothermal route without the assistance of any template molecule. As-prepared composite was characterised by SEM, TEM, HRTEM, XRD, XPS for surface features, morphological and crystalline characters. The formed nanostructures were determined to possess crystal-like geometrical shape and average size less than 100 nm. The as-synthesised nanocomposite was further investigated for their heterogeneous photocatalytic potential against the oxidative degradation of CV dye taken as model pollutant. The photo-catalytic performance of the as-synthesised material was evaluated both under ultra-violet as well as visible light. Best photocatalytic performance was achieved under visible light with complete degradation (100%) exhibited within 60 min of irradiation time. The kinetics of the photocatalytic process were also considered and the reaction rate constant for CeO_2–TiO_2 nanocomposite was determined to be 0.0125 and 0.0662 min^{-1} for ultra-violet and visible region, respectively. In addition, the as-synthesised nanocomposite demonstrated promising results when considered for the photo-catalytic degradation of coloured industrial waste water collected from local textile industry situated in Faisalabad region of Pakistan. Enhanced photo-catalytic performance of CeO_2–TiO_2 nanocomposite was proposed owing to heterostructure formation leading to reduced electron–hole recombination.

Keywords CeO_2–TiO_2 nanocomposite · Heterogeneous photocatalysis · Degradation of crystal violet · Environmental remediation

Introduction

All domestic, commercial and industrial activities involve the use of water as a most important and basic need; moreover, the wastewater generated as a result of such activities can pose enormous hazards to the environment because of contaminants introduced into water systems. The textile, paper, paint and many other industries use dyes in colouring their products for finishing, consuming large volumes of water and releasing effluents containing various forms of recalcitrant contaminants which pose a threat to aquatic life (Mallick et al. 2005; Das et al. 2011; Abdulla-Al-Mamun et al. 2009). The literature describes that in terms of both volume and effluent constitution, the wastewater discharged by the textile industry have been rated as one of the most polluting sources among all industrial divisions (Wang et al. 2010). Therefore, many countries have implemented new and strict regulations imposing strong obligatory measures

✉ Waheed S. Khan
waheedskhan@yahoo.com; waheedskhan@nibge.org

1 National Institute for Biotechnology and Genetic Engineering (NIBGE), Jhang Road, Faisalabad 38000, Pakistan

2 National Centre for Physics, QAU Campus, Shahdra Valley Road, Islamabad 44000, Pakistan

3 Division of Science and Technology, University of Education, College Road Township, Lahore, Pakistan

4 Nanobiomaterials Group, Ningbo Institute of Materials Technology and Engineering (NIMTE), Chinese Academy of Sciences (CAS), Ningbo, Zhejiang, People's Republic of China

regarding wastewater disposal during the last decade (He et al. 2012). The literature also demonstrates how conventional methods have been found to be ineffective, cumbersome and expensive to make water systems clean and safe (Rauf et al. 2011). However, reports also show that the great difficulty in treating dye-containing wastewater is the ineffectiveness of biological processes (Lu et al. 2011; Bokare et al. 2008; Poulios et al. 2003; Ma et al. 2002). While the physical processes, such as coagulation and adsorption, simply transfer the pollutants from one medium to another and cause secondary pollution to the environment and aquatic life. The conventional oxidation processes like ozonation and chlorination are limited to some classes of dyes (Mallick et al. 2005; Wang et al. 2010). It is also described that due to the earlier mentioned difficulties in treating wastewaters, broad research interest has been shown in the application of advanced oxidation processes (AOPs) to treat organic chemicals including dyes and other pollutants. Among several AOPs, heterogeneous photo-catalysis concerning semiconductors has held significant attention in the recent years for the remediation of detrimental pollutants both in aqueous and gaseous phases using solar or artificial light sources (Soomro and Nafady 2015). These are utilised as efficient and low cost-effective procedures for removing stable organic compounds including dye molecules. The other advantage of heterogeneous photo-catalysis is that the catalyst recycling would make the remediation process less expensive (Abdul et al. 2016).

Among all semiconductor photocatalysts being used in water treatment, anatase TiO_2, with the band energy of 3.2 eV is found to reveal a desirable photocatalytic activity under UV light irradiation. However, pure TiO_2 has a wide band gap which limits its utility in wider range of spectrum. Thus, to improve photocatalytic activity, designing of coupled semiconductor heterojunction is a promising approach. To date, various nanocomposite of TiO_2 coupled with other materials such as ZnO (Murugan et al. 2013), Fe_3O_4-/CuO-/TiO_2-/Ag-nanocomposite (Fauzian et al. 2017), CeO_2 (Liu et al. 2017) and Cu_2O (Zhen et al. 2017) have been reported to improve the charge separation and broadening the photoresponse region. In this regard, the use of CeO_2 is getting significant scientific interest due to its suitable band-gap position (Barton et al. 2015) and the high capacity to store/release oxygen under oxidising/reducing conditions of CeO_2 (Verma et al. 2015). The combination of CeO_2 with TiO_2 as nanocomposite can result in promising photo-catalytic activity based on reversible conversion between Ce(IV) and Ce(III) that would allow proficient electron transfer between the two constituents. Thus, in this present study we report the synthesis of template-free CeO_2-doped TiO_2 nanocomposite using simple hydrothermal approach. The study further explores the potential of as-synthesised nanocomposite as a heterogeneous and recyclable photo-catalyst which produces highly enhanced photo-degradation of common textile dye (i.e., CV). The dye has been used as model compound to monitor the catalytic efficiency of the as-synthesised nanocomposite. The results obtained from catalytic performance of CeO_2-doped TiO_2 at optimum conditions showed 97% degradation of CV dye in only 60 min. Comparative degradation studies were carried under both UV and visible light. Moreover, the as-synthesised material demonstrated excellent working capabilities when used for the photo-catalytic degradation of real textile waste water samples collected from local textile industries of Faisalabad region Pakistan. In addition, we suggest that the results obtained in this present research can be extended to degrade many other organic dyes and low molecular weight organic/inorganic compounds, which pose substantial hazardous effects and toxicity to the aqueous environment.

Materials and methods

The nanocomposite was synthesised using hydrothermal route. In a typical experiment, 0.2 g of CeO_2 powder (ACROS Organics with 99.9% purity) was allowed to vortex with 0.4 g of commercial TiO_2 powder (Sigma Aldrich, 99.9%) in 150 ml of KOH (1 M). The pH of the solution was maintained at 10 followed by hydrothermal treatment in Teflon lining autoclaved at 180 °C for 24 h. After completion of the reaction, the nanocomposite was separated from the reactor using high-speed centrifugation at 3000 rpm. The as-synthesised nanocomposite was thoroughly washed with de-ionised water and ethanol to remove any surface bound impurity. The nanocomposite was then finally dried at 60 °C for 6 h before utilising them as an active photo-catalytic material.

Characterization

Morphological and structural characterisation was carried using field-emission scanning electron microscopy FESEM-JEOL (JSM-7500F), Transmission Electron Microscope (FEI Tecnai F20), and X-ray diffraction (XRD) (Bruker D-8). X-ray photoelectron spectroscopy (XPS) measurements were made using an Omicron Nanotechnology GmbH with Al Kα (1486.6 eV) as the X-ray source. The photo-catalytic activity was carried under 200 W incandescent light bulb and UV lamp (Camag, Switzerland) for visible and ultra-violet studies. The monitoring of the photo-catalytic activity was measured using UV–Vis spectrophotometer (CECIL-7000).

The photo-catalytic performance of the as-synthesised nanocomposite

Photo-catalytic activity of newly synthesised nanocomposite in removing contaminants from aqueous media was checked using CV dye as a test contaminant. In a typical batch test, a specific amount of nanocomposite was allowed to vortex with 75-ml CV solution (24.5 mM) for 60 min in dark (without light irradiation) to obtain the maximum adsorption/desorption of dyes on the catalyst surface. To monitor the photo-catalytic performance, the mixture of dye, photocatalyst and oxidant (H_2O_2) was exposed to UV and visible lights for corresponding irradiations. The degradation efficiency was followed by collecting aliquots of the sample and measuring the decline in maximum absorbance (λ_{max}) of CV at 583 nm. To ensure proper measurement, the collected samples were filtered using 0.45-µm membrane filters to remove any suspended particles.

Results and discussion

Structural characterization

The as-synthesised nanocomposite was elaborately characterised for their morphology, composition and structural characteristics using SEM, TEM, HRTEM, XRD and XPS. Figure 1a shows the SEM micrograph of the as-synthesised product and indicates the formation of small crystal-like nanosized particles. The formed nanostructures are evident to possess different geometrical like shapes such a triangular, circular, rectangular, hexagonal, etc. The average size of the as-synthesised nanoparticles was determined to be less than 100 nm as indicated in TEM image Fig. 1b. HRTEM image shown in Fig. 1c reflects the single crystalline character of the CeO_2–TiO_2 nanocomposite with clear lattice fringes.

The XRD pattern recorded for the as-synthesised nanocomposite is shown in Fig. 1d. The XRD consists of peaks indexed to (101), (111), (200), (004), (112), (220), (200), (105), (311), (222) planes of CeO_2 and TiO_2 as standardised against the ICCD no. 34-0394 and 21-1272, respectively. The absence of any other peaks is evident of product purity.

To ensure the surface purity of the as-synthesised nanocomposite, XPS analysis was performed. Figure 2 shows the wide scale spectrum for CeO_2–TiO_2 nanocomposite with integrated major peaks inferred to C 1*s*, O 1*s*, Ti 2*p* and Ce 3*d*, respectively. The full scan was further regionalized to provide information of specific binding energies associated with ceria and titania (Fig. 2a). The O 1*s* spectrum is shown in Fig. 2b). The two major peaks are evident of two types of oxygen species present on the sample surface. The peak at 531.1 eV is attributed to the surface-lattice oxygen whereas

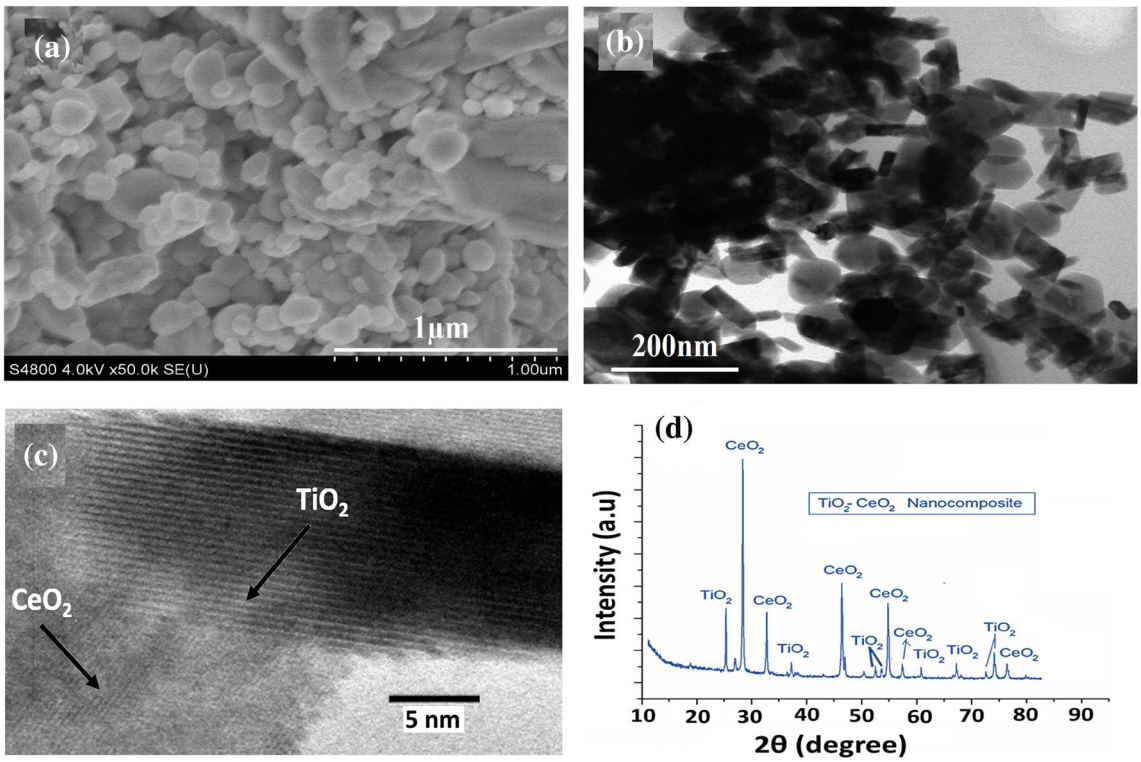

Fig. 1 **a** SEM micrograph; **b** TEM image; **c** HRTEM image and **d** XRD pattern of the as-synthesised CeO_2–TiO_2 nanocomposite

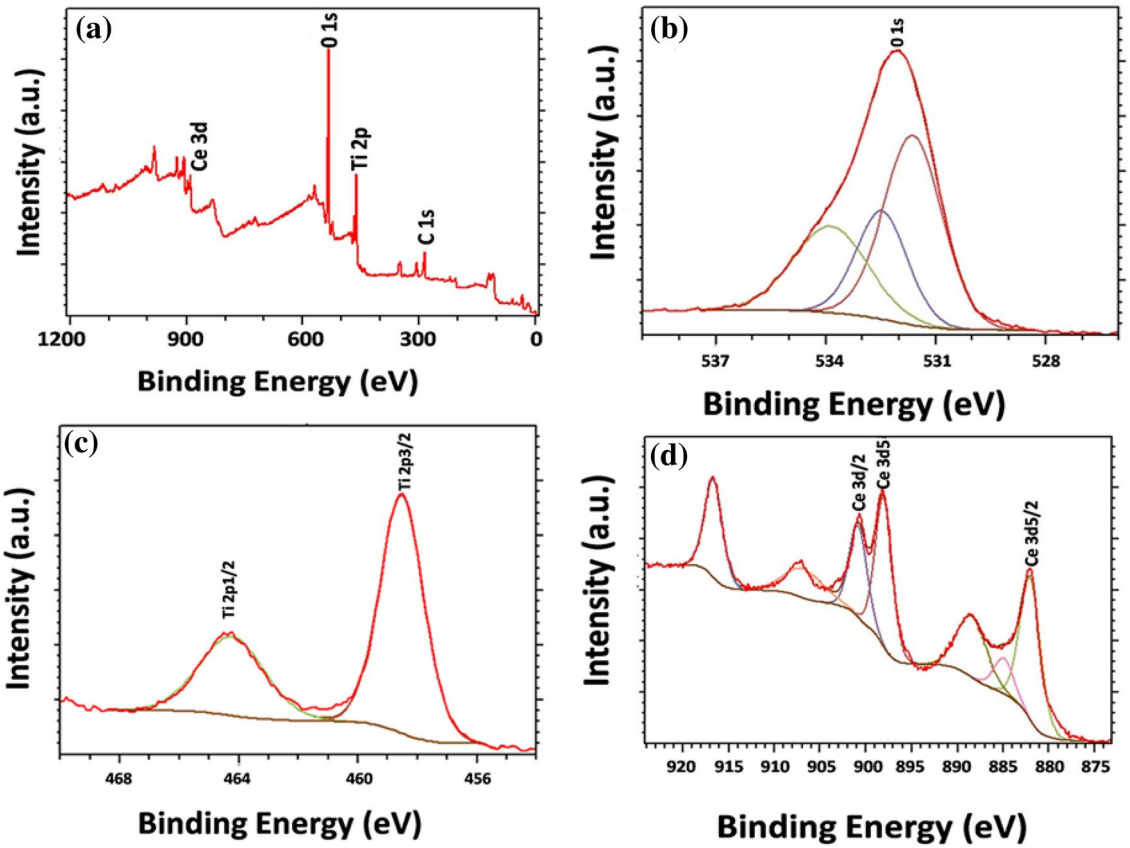

Fig. 2 **a** XPS, full scan of CeO_2–TiO_2 nanocomposite. **b** XPS O 1*s* data for CeO_2 nanoparticles. **c** XPS Ti 2*p* data for CeO_2@TiO_2. **d** XPS Ce 3*d* data for CeO_2–TiO_2 nanocomposite

the peak at 534.4 eV is from the oxygen that is chemisorbed as –OH/–CO_3^{2-} or adsorbed water. Figure 2c shows the binding energies of Ti $2p^{3/2}$ and $2p^{1/2}$ from CeO_2–TiO_2. The peaks observed at the 458.65 and 464.36 eV are evident of the presence of Ti species with CeO_2. The Ce 3*d* spectra in Fig. 2d were fitted using eight peaks, where $3d^{3/2}$ and $3d^{5/2}$ are spin-orbital.

Evaluation of photo-catalytic performance

The CeO_2–TiO_2 nanocomposite with its higher surface area and small crystal size was expected to demonstrate high photo-catalytic performance. The photo-catalytic performance was evaluated both under visible and ultra-violet light. Figure 3a shows the un-catalysed reaction which was carried out to assess the capability of the oxidant (H_2O_2) alone for the degradation of CV dye (0.024 M).

The slight degradation up to 13% signifies the incapability of the oxidant to completely degrade the dye molecules as shown in Fig. 3a. In contrast, the catalyst reaction carried out in the ultra-violet light demonstrates significant degradation of CV dye in the given time of 60 min. The gradual decrement in the absorbance intensity at $\lambda_{max} = 580$ nm CeO_2–TiO_2 nanocomposite is a clear evidence of uniform photo-catalytic reaction. The use of CeO_2–TiO_2 nanocomposite as photo-catalyst under ultra-violet light led to 65% degradation within the 60 min of reaction time as indicated in Fig. 3b. Contrary to this, the use of visible light source at the same experimental conditions resulted in 100% degradation of CV within 60 min of reaction time as exhibited in Fig. 3c. This variation in the catalytic performance of CeO_2–TiO_2 nanocomposite is attributed to photo-active band gap of CeO_2–TiO_2 nanocomposite that allows greater generation of electron–hole pairs which coupled with high surface area of composite leading to enhanced degradation kinetics.

The rate of heterogeneous photo-catalytic reaction is best estimated using Langmuir–Hinshelwood (L–H) model (Houas et al. 2001), which has the following mathematical formula (Sun et al. 2002):

$$-\frac{dc}{dt} = \frac{k_{L-H} k_{ad} C}{1 + k_{ad} C}, \quad (1)$$

where k_{L-H} is the reaction rate constant, k_{ad} is the adsorption coefficient of CV dye over the catalyst, and C is the distinct

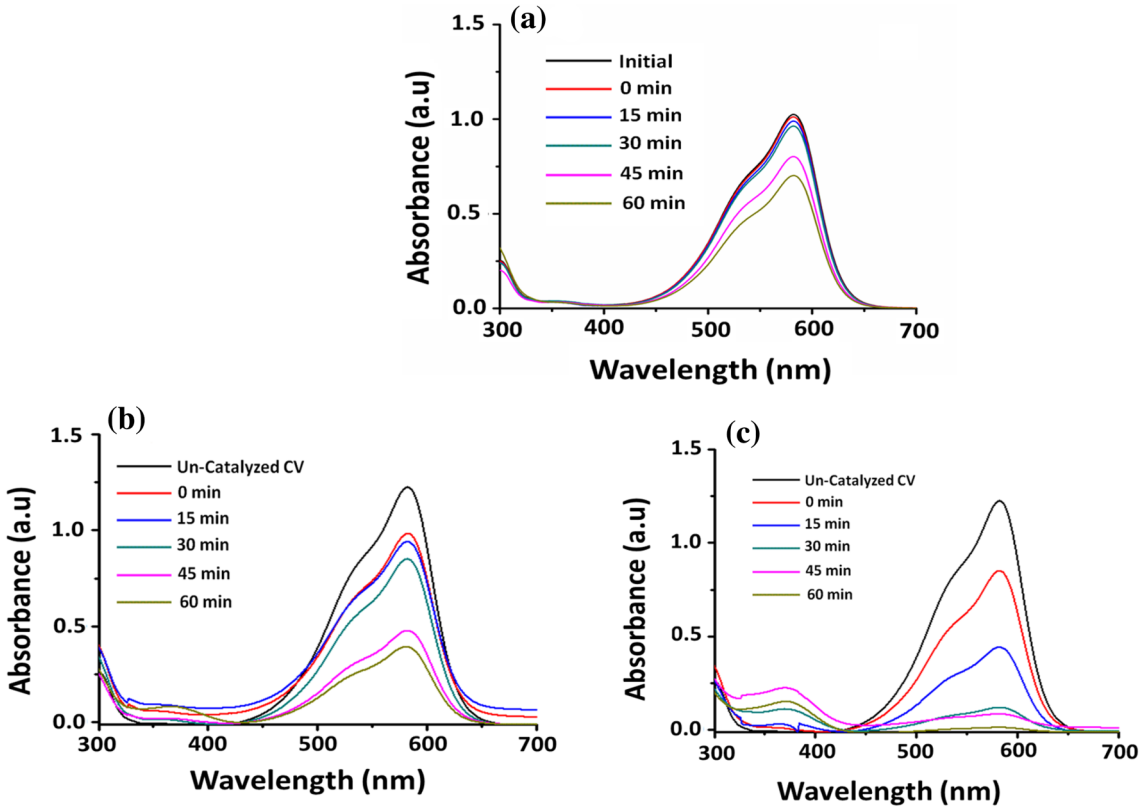

Fig. 3 UV–Vis spectral profile for **a** un-catalysed for 0.024 M CV dye with 500 µL H_2O_2; photo-catalytic degradation of CV under **b** ultra-violet and **c** visible light

concentration at any time t. Since, the value of k and C are very small for pseudo-first-order reactions, so Eq. (1) can be simplified to Eq. (2):

$$\ln\left(\frac{C_0}{C}\right) = k_{\mathrm{L-H}}k_{\mathrm{ad}}t = -kt. \tag{2}$$

Here C_0 is the initial concentration and $k = k_{\mathrm{L-H}}\, k_{\mathrm{ad}}$ is the pseudo-first-order reaction rate constant.

Figure 4 shows the plot of linear relationship between the natural logarithm of ratio of initial concentration (C_0) of CV and relative remaining concentration (C) after oxidative degradation versus the corresponding reaction time (s). The linear regression analysis was used to estimate the degradation constant under UV light (Fig. 4a) as well as visible light (Fig. 4b). The k value for CeO_2–TiO_2 nanocomposite under ultra-violet light is 0.0125 whereas for visible light 0.0662 min^{-1} was observed, respectively. The high value of k in case of visible light signifies the favourable reaction rate following pseudo-first-order kinetics. To ensure maximum degradation, the amount of photocatalyst was optimised in the range of 0.01–0.02 mg/ml. Figure 4c shows the variation of degradation efficiency against the catalyst dose. An initial increment is evident of the higher surface area provided by greater density of CeO_2–TiO_2 nanocomposite. The maximum degradation was achieved using 15 mg/ml whereas at the higher dose, saturation condition was observed.

The photo-catalytic degradation was further validated by analysing the post-treated samples using high-performance liquid chromatography–electrospray ionisation (HPLC–ESI) mass spectrometry, and the relevant mass spectra are illustrated in Fig. 5. The molecular ion peaks appeared in the protonated forms of the intermediates. As shown in Fig. 5a, the spectral analysis confirmed that *m/z* 372.2 in liquid chromatogram is CV. After degradation as in Fig. 5b, it shows different peaks which indicate the degradation of CV dye. Previous reports depict that CV dye degradation occurred by *N*-de-methylation reaction. (i.e., band wavelength shift toward blue region is because of methyl group removal) (Chen et al. 2007).

Photo-catalytic degradation of real-coloured waste water

The universality of CeO_2–TiO_2 based nanocomposite as a photo-catalyst was examined by utilising the material for the degradation of real-coloured waste water samples. A

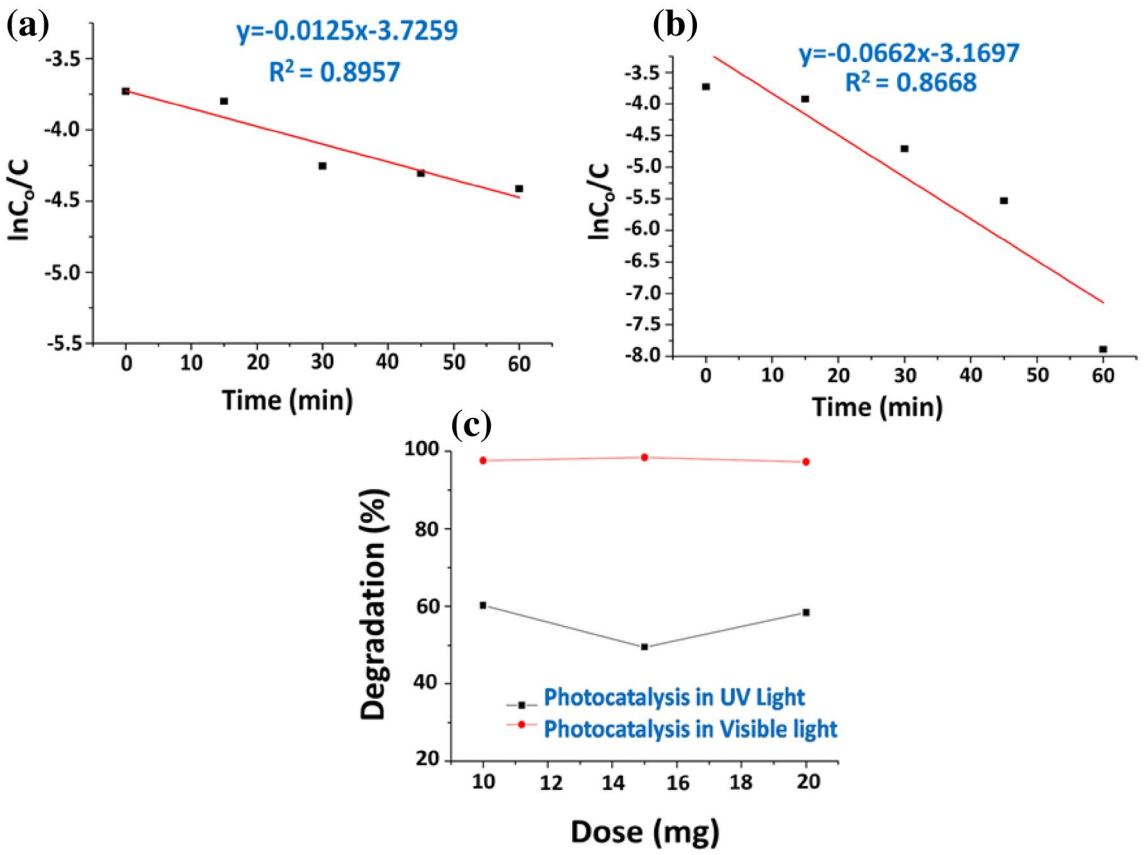

Fig. 4 **a**, **b** Linear regression plot for pseudo-first-order kinetics for the nanocomposite catalysed oxidative degradation of CV under ultraviolet and visible spectrum of light; **c** variation in the % degradation efficiency in reference to standard dosage of photo-catalyst

sample of coloured waste water was collected from local textile industry situated in the Faisalabad region of Pakistan. The sample was filtered and properly diluted before subjecting it for photo-catalytic degradation. The photocatalysis was carried in similar fashion as mentioned in "Evaluation of photo-catalytic performance", however, the amount of oxidant was raised to 1 ml due to the complex nature of the coloured sample. Figure 6a shows the UV–Vis spectrum of the sample before treatment whereas Fig. 6b exhibits UV–Vis spectra after treatment. The complete degradation of the coloured sample is evident from the constant decline of the spectral peak intensities.

Photo-catalytic efficiency of the as-synthesised CeO_2–TiO_2 nanocomposite for CV dye degradation was compared with various other photo-catalysts used for the degradation of CV dye as shown in Table 1.

Figure 7 presents the proposed mechanism of CV dye degradation by CeO_2–TiO_2 nanocomposite catalyst. The picture shows that the energy band gap of titania (3.10 eV) is larger than that of ceria (2.74 eV) (Tian et al. 2013; Fan et al. 2016; Lu et al. 2016). The energy level of the conduction band of ceria is lower (more negative) than titania. Conversely, the energy level allows faster transfer of the holes from titania to ceria (Wang et al. 2011).

Finally, the complete separation of electron–hole pairs results in increased generation of $O^{2\cdot-}$ and hydroxyl radical resulting in improvement of the photocatalytic activity of the CeO_2–TiO_2 nanocomposite catalyst. This synergistic effect of CeO_2–TiO_2 nanocomposite photocatalyst displays a higher photocatalytic activity than separate TiO_2 and CeO_2 photocatalysts under visible light irradiation (Eskandarloo et al. 2014).

Conclusion

In conclusion, this study explores the potential of CeO_2–TiO_2 nanocomposite synthesised using simple hydrothermal route for the photo-catalytic degradation of common textile dye namely CV. The as-synthesised nanocomposites were examined for their photo-catalytic activity both under ultra-violet and visible light. The as-synthesised nanocomposite demonstrated potential photo-catalytic activity against the target dye where maximum

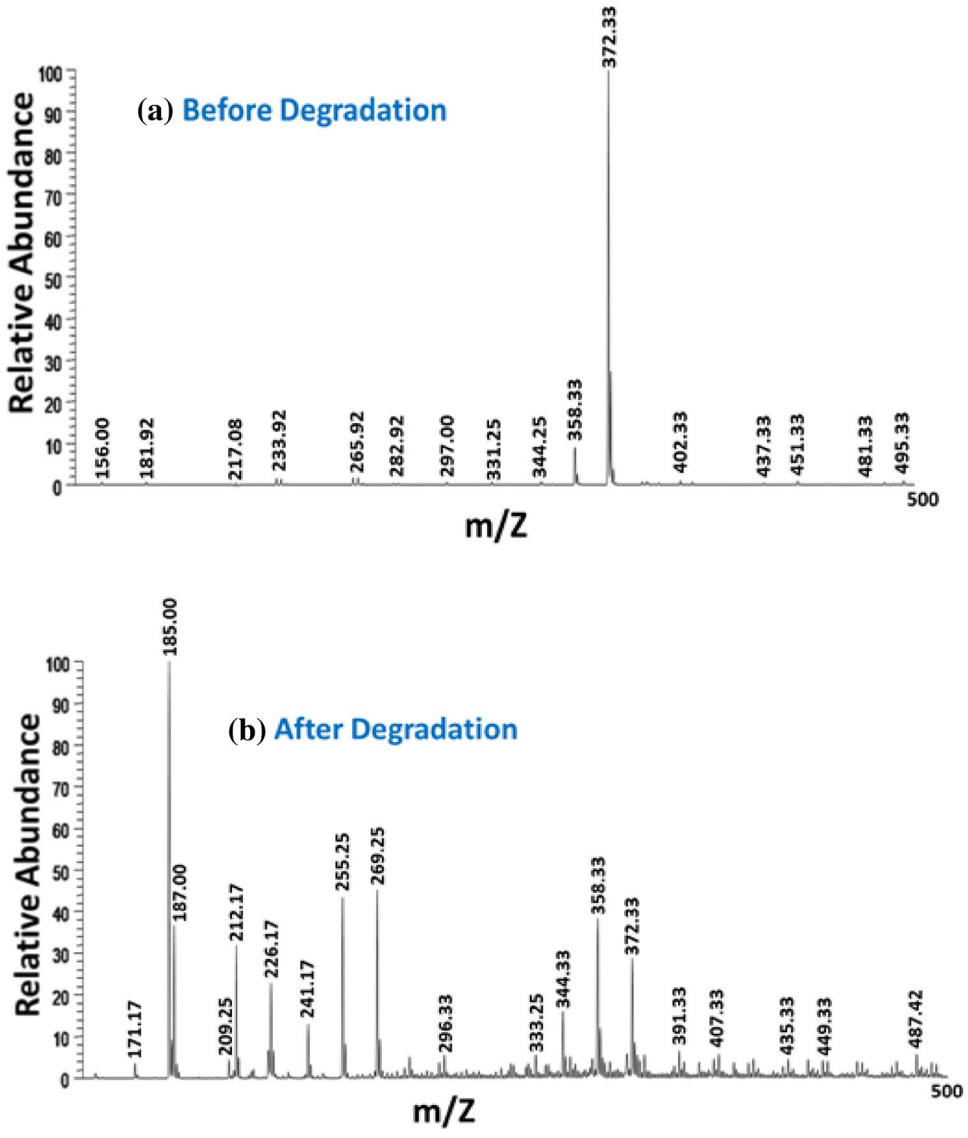

Fig. 5 ESI mass spectra of CV dye **a** before degradation. **b** After degradation showing multiple intermediates

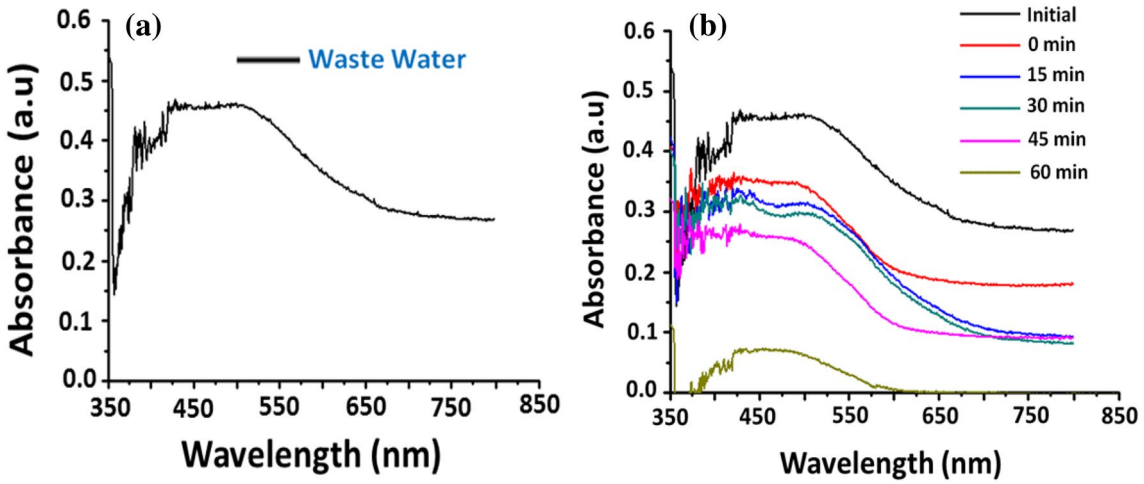

Fig. 6 UV–Vis spectra profile for the **a** un-catalysed **b** catalysed waste water sample

Table 1 Comparison of CV dye degradation using ceria–titania nanocomposite with other materials

Catalyst	Efficiency (%)	Irradiation source	Time	References
Anatase nanosphere TiO_2	99	UV light	6 h	Jadhav et al. (2013)
Mn doped and PVP capped ZnO NPs	< 100	UV irradiation	3 h	Mittal et al. (2014)
TG capped ZnS NPs	~ 96	UV–visible irradiation	3 h	Sharma et al. (2012)
CeO_2–TiO_2 nanocomposite	~ 98	Visible light	60 min	Present

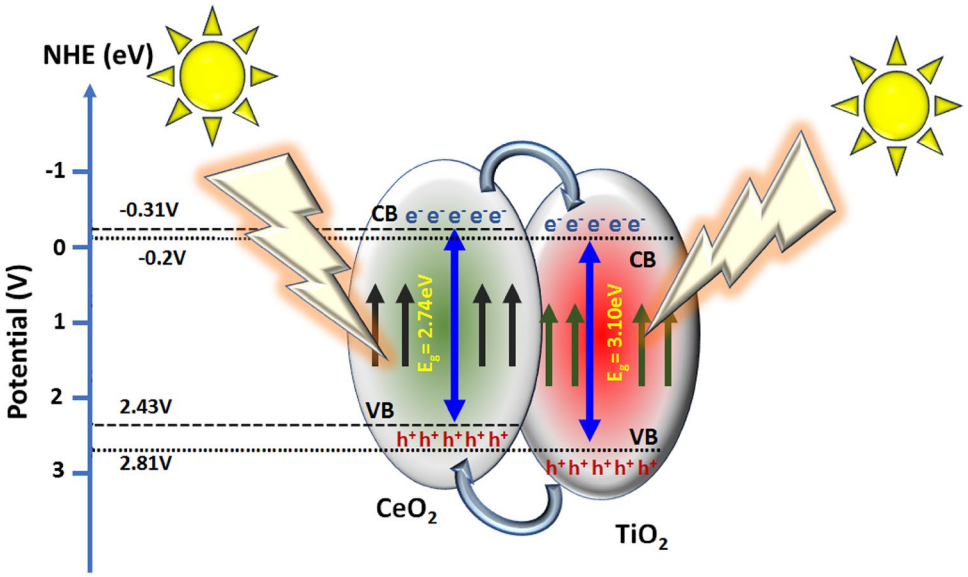

Fig. 7 Proposed photocatalytic degradation mechanism of CV using CeO_2–TiO_2 nanocomposite under visible light irradiation

degradation was achieved just within 60 min of reaction time under visible light. The efficient catalytic potential in case of CeO_2–TiO_2 nanocomposite can be attributed to the high surface area and favourable band gap condition due to synergetic combination of Ce and Ti species. The kinetics of photo-catalytic process was also evaluated using Langmuir–Hinshelwood (L–H) model where the rate constant of 0.0125 and 0.0662 min^{-1} were determined for ultra-violet and visible region. Moreover, the system demonstrated working capability against real waste water effluent collected from local textile industry situated in Faisalabad region of Pakistan.

Acknowledgements This research is funded by Higher Education Commission (HEC) of Pakistan by research Grant no. NRPU6115. Dr. Waheed S. Khan also acknowledges the support of Chinese Academy of Sciences under CAS-PIFI Fellowship at Ningbo Institute of Materials Technology and Engineering (NIMTE), Ningbo City, Zhejiang, P. R. China.

Compliance with ethical standards

Conflict of interest There are no conflicts of interest to declare.

References

Abdul RK, Saba N, Razium AS, Faruk ÖAA, Nazar HK, Abdul WM, Imren HP, Mustafa E (2016) L-Lysine derived nickel nanoparticles for reductive degradation of organic dyes. Adv Mater Lett 7(8):616–621

Abdulla-Al-Mamun M, Kusumoto Y, Muruganandham M (2009) Simple new synthesis of copper nanoparticles in water/acetonitrile mixed solvent and their characterization. Mater Lett 63(23):2007–2009

Barton LE, Auffan M, Olivi L, Bottero J-Y, Wiesner MR (2015) Heteroaggregation, transformation and fate of CeO_2 nanoparticles in wastewater treatment. Environ Pollut 203:122–129

Bokare AD, Chikate RC, Rode CV, Paknikar KM (2008) Iron-nickel bimetallic nanoparticles for reductive degradation of azo dye orange G in aqueous solution. Appl Catal B 79(3):270–278

Chen C-C, Mai F-D, Chen K-T, Wu C-W, Lu C-S (2007) Photocatalyzed *N*-de-methylation and degradation of crystal violet in titania dispersions under UV irradiation. Dyes Pigment 75(2):434–442

Das R, Nath SS, Bhattacharjee R (2011) Luminescence of copper nanoparticles. J Lumin 131(12):2703–2706

Eskandarloo H, Badiei A, Behnajady MA (2014) TiO_2/CeO_2 hybrid photocatalyst with enhanced photocatalytic activity: optimization of synthesis variables. Ind Eng Chem Res 53(19):7847–7855

Fan Z, Meng F, Gong J, Li H, Hu Y, Liu D (2016) Enhanced photocatalytic activity of hierarchicalflower-like CeO_2/TiO_2 heterostructures. Mater Lett 175:36–39

Fauzian M, Taufik A, Saleh R (2017) Synthesis, characterization and visible light photocatalytic of $Fe_3O_4/CuO/TiO_2$/Ag nanocomposites. IOP conference series: materials science and engineering. IOP Publishing, Bristol. p 012009

He Y, Gao J-F, Feng F-Q, Liu C, Peng Y-Z, Wang S-Y (2012) The comparative study on the rapid decolorization of azo, anthraquinone and triphenylmethane dyes by zero-valent iron. Chem Eng J 179:8–18

Houas A, Lachheb H, Ksibi M, Elaloui E, Guillard C, Herrmann J-M (2001) Photocatalytic degradation pathway of methylene blue in water. Appl Catal B 31(2):145–157

Jadhav V, Dhabbe R, Sabale S, Nikam G, Tamhankar B (2013) Degradation of dyes using high temperature stable anatase nanosphere TiO_2 photocatalyst. Univ J Environ 3(6):667–676

Liu Z, Yu Q, Liu J, Li T, Huang F (2017) Enhanced visible photocatalytic activity in flower-like $CuO–WO_3–Bi_2WO_6$ ternary hybrid through the cascadal electron transfer. Micro Nano Lett 12(3):195–200

Lu X, Zhang B, Wang Y, Zhou X, Weng J, Qu S, Feng B, Watari F, Ding Y, Leng Y (2011) Nano-Ag-loaded hydroxyapatite coatings on titanium surfaces by electrochemical deposition. J R Soc Interface 8(57):529–539

Lu X, Li X, Qian J, Miao N, Yao C, Chen Z (2016) Synthesis and characterization of CeO_2/TiO_2 nanotube arrays and enhanced photocatalytic oxidative desulfurization performance. J Alloy Compd 661:363–371

Ma L, Wang X, Wang B, Chen J, Wang J, Huang K, Zhang B, Cao Y, Han Z, Qian S (2002) Photooxidative degradation mechanism of model compounds of poly(*p*-phenylenevinylenes) [PPVs]. Chem Phys 285(1):85–94

Mallick K, Witcomb MJ, Scurrell MS (2005) Preparation and characterization of a conjugated polymer and copper nanoparticle composite material: a chemical synthesis route. Mater Sci Eng B 123(2):181–186

Mittal M, Sharma M, Pandey O (2014) Photocatalytic studies of crystal violet dye using Mn doped and PVP capped ZnO nanoparticles. J Nanosci Nanotechnol 14(4):2725–2733

Murugan R, Babu V, Khin MM, Nair A, Ramakrishna S (2013) Synthesis and photocatalytic applications of flower shaped electrospun $ZnO–TiO_2$ mesostructures. Mater Lett 97:47–51

Poulios I, Micropoulou E, Panou R, Kostopoulou E (2003) Photooxidation of eosin Y in the presence of semiconducting oxides. Appl Catal B 41(4):345–355

Rauf M, Meetani M, Hisaindee S (2011) An overview on the photocatalytic degradation of azo dyes in the presence of TiO_2 doped with selective transition metals. Desalination 276(1):13–27

Sharma M, Jain T, Singh S, Pandey O (2012) Photocatalytic degradation of organic dyes under UV–visible light using capped ZnS nanoparticles. Sol Energy 86(1):626–633

Soomro RA, Nafady A (2015) Catalytic reductive degradation of methyl orange using air resilient copper nanostructures. J Nanomater 16(1):120

Sun Z, Chen Y, Ke Q, Yang Y, Yuan J (2002) Photocatalytic degradation of a cationic azo dye by TiO_2/bentonite nanocomposite. J Photochem Photobiol A 149(1):169–174

Tian J, Sang Y, Zhao Z, Zhou W, Wang D, Kang X, Liu H, Wang J, Chen S, Cai H (2013) Enhanced photocatalytic performances of CeO_2/TiO_2 nanobelt heterostructures. Small 9(22):3864–3872

Verma R, Samdarshi S, Singh J (2015) Hexagonal ceria located at the interface of anatase/rutile TiO_2 superstructure optimized for high activity under combined UV and visible-light irradiation. J Phys Chem 119(42):23899–23909

Wang K-S, Lin C-L, Wei M-C, Liang H-H, Li H-C, Chang C-H, Fang Y-T, Chang S-H (2010) Effects of dissolved oxygen on dye removal by zero-valent iron. J Hazard Mater 182(1):886–895

Wang J, Guo Y, Liu B, Jin X, Liu L, Xu R, Kong Y, Wang B (2011) Detection and analysis of reactive oxygen species (ROS) generated by nano-sized TiO_2 powder under ultrasonic irradiation and application in sonocatalytic degradation of organic dyes. Ultrason Sonochem 18(1):177–183

Zhen W, Jiao W, Wu Y, Jing H, Lu G (2017) The role of a metallic copper interlayer during visible photocatalytic hydrogen generation over a $Cu/Cu_2O/Cu/TiO_2$ catalyst. Catal Sci Technol 7(21):5028–5037